CERN-ATS-Note-2011-057 MD (LHC)

03.07.2011
Florian.Burkart@cern.ch
Daniel.Deboy@cern.ch
Daniel.Wollmann@cern.ch

Beam distribution measurements in the LHC

R.W. Assmann, R. Bruce, F. Burkart, M. Cauchi, D. Deboy, L. Lari, S. Redaelli, A. Rossi, G. Valentino, D. Wollmann, CERN, Geneva, Switzerland

Keywords: Collimation, Beam halo

Summary

Understanding the population and shape of the beam halo is important to predict possible intensity limitations due to collimation at 7 TeV. Therefore studies to measure the population of the beam halo are indispensable. Furthermore, using horizontal, vertical and skew collimators during halo scans opens the possibility to confirm the results measured in single plane scans. During the beam distribution MD in the LHC one set of slow full beam scrapings (hor., ver. and skew) with a step size of 40 μm was performed at 450 GeV in both beams. In addition fast full beam scrapings with the vertical primary collimators in IR7 were conducted.
In this note the results of the different measurements are presented and compared.

1 INTRODUCTION

During physics operation at 3.5 TeV the lowest beam lifetimes and therefore the highest losses at primary collimators appear when the two LHC beams are brought into collision [1]. These losses are mainly caused by a reduction of the dynamic aperture, which causes a cleaning out of the concerned beam halo regions. As this could become a limit for the intensity in the LHC at 7 TeV it is important to measure the population and shape of the beam halo.

Previous measurements were performed either as fast full beam scrapings or as end of fill experiments with high intensity physics beams. Without a high frequency beam intensity signal from the FBCTs the upper measurements were strongly limited in their spacial resolution, due to the standard 1 Hz FBCT signal and the 2 mm/s speed of the collimator jaw movement. Whereas in the latter only a small part of the beam halo could be scraped away, as the beams where dumped when the losses reached the BLM dump thresholds.

Therefore beam halo studies in the LHC at 450 GeV using the horizontal, vertical and skew primary collimators of each beam were performed during the second LHC-MD block in 2011. Furthermore, during the beam scrapings the signals from two condenser microphones

Table 1: Measured normalized emittance of the two beams before the respective beam scrapings.

Scraping	$\epsilon_{h,B1}$ $[\mu m]$	$\epsilon_{v,B1}$ $[\mu m]$	$\epsilon_{h,B2}$ $[\mu m]$	$\epsilon_{v,B2}$ $[\mu m]$
slow vertical (TCP.D)	1.4	1.4	1.8	1.9
slow horizontal (TCP.C)	1.4	1.2	1.7	1.7
slow skew (TCP.B)	1.3	1.3	1.9	2.1
fast vertical (TCP.D)	1.8	1.7	2.6	2.9

installed close to the IR7 primary collimators in beam 1 were recorded.

In this paper the measured population of the beam halo in the different planes and the analysis of the microphone data are presented and discussed.

2 MD programm

During the beam distribution MD it was planned to measure:

- three full sets of slow beam scrapings, i.e. in the horizontal, vertical and skew planes, with different step sizes for the collimator jaw movement and one nominal bunch per beam at 450 GeV.
- one full set of slow beam scrapings with physics beam ($\sim$ 1380 bunches) at 450 GeV;
- one full set of fast beam scrapings with one nominal bunch per beam at 450 GeV;
- one vertical scrapings per beam with one nominal bunch at 3.5 TeV.

As the LHC was only available during about 1h45mins of the planned 4h for the measurements, only a minimal subset of measurements could be performed:

- one full set of slow beam scrapings with a step size of 40 μm repeated every 4 seconds and one nominal bunch ($\sim 1.1e11$ p) per beam at 450 GeV.
- one vertical fast beam scraping per beam with one nominal bunch at 450 GeV.

Figure 1 shows the beam intensity during the MD. The different scraping experiments are labelled in the plot. The measured normalized beam emittance at the beginning of the different fills during the experiment are listed in table 1. Figure 2 shows the normalized instantaneous loss rates versus the collimator half gap for the set of slow scrapings in B1 and B2.

3 MD Results

3.1 Slow scraping

The slow beam scrapings were performed with a step size of 40 μm every 4 seconds. From figure 1 it can be seen that B1 and B2 were scraped away in parallel with a delay of 2 seconds between the movement of the respective primary collimators.

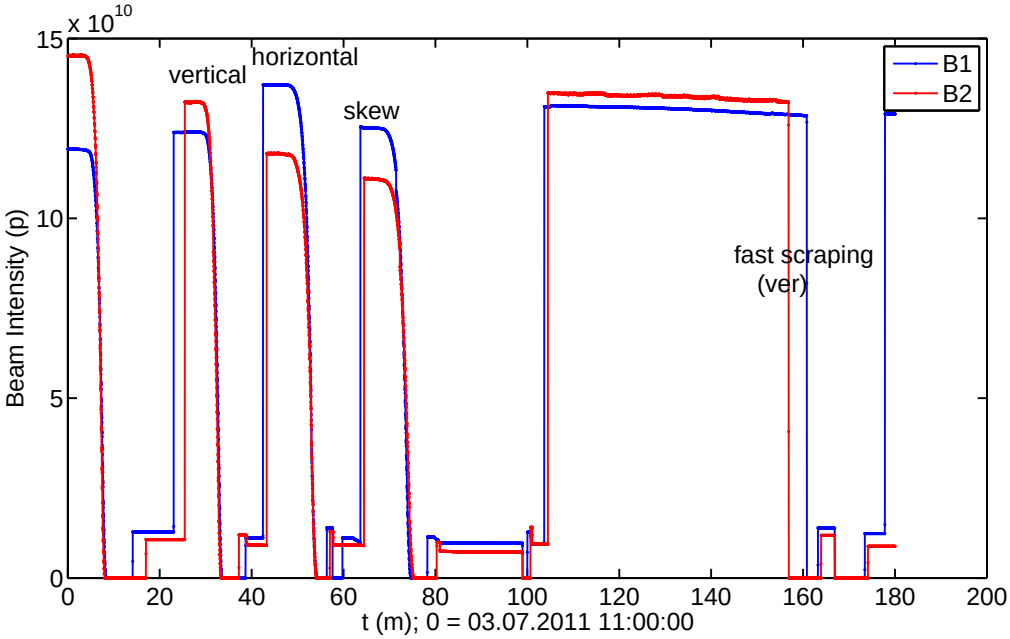

Figure 1: Intensity in B1 and B2 during the MD. The fast and slow full beam scrapings are labelled in the plot accordingly.

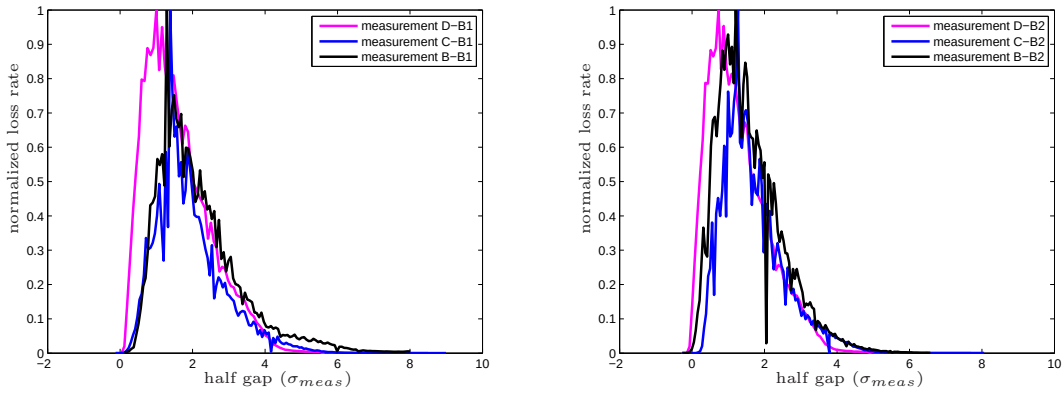

Figure 2: Normalized instantaneous loss rates during the scraping experiments in B1 (**left**) and B2 (**right**) versus the collimator half gap in units of measured beam size, σ_{meas}. The scrapings were performed in the vertical (purple), horizontal (blue) and skew plane (black) with the respective primary collimators in IR7: D- ver, C-hor and B-skew.

Table 2: Overview of the calibration factors f^i_{calib} achieved from correlating the BLM signals, S^i_{blm}, to the beam intensity signals from the fast beam current transformers (FBCT) for the different slow scraping experiments.

Scraping	f^i_{calib} [p/Gy] B1	f^i_{calib} [p/Gy] B2
slow vertical (TCP.D)	1.2×10^{12}	1.13×10^{12}
slow horizontal (TCP.C)	1.25×10^{12}	1.26×10^{12}
slow skew (TCP.B)	1.94×10^{12}	1.75×10^{12}

The instantaneous loss rate at the respective collimator i can then be calculated as

$$R_i(t) = f^i_{calib} S^i_{blm}(t). \tag{1}$$

The calibration factors f^i_{calib} were achieved by correlating the BLM signals, S^i_{blm}, to the beam intensity signals from the fast beam current transformers (FBCT). Table 2 lists the calibration factors for the different slow scrapings. With one step every 4 seconds and the publishing frequency of the BLM signals of 1 Hz the lost intensity at each collimator jaw position u is given as

$$I_L(u) = \sum_{j=1}^{4} \left(R_i(t_{u,j}) \cdot 1s \right). \tag{2}$$

The intensity left over in the beam at each collimator jaw position u can then be written as

$$I(u) = \sum_{u}^{u_{end}} I_L(u) = \sum_{u}^{u_{end}} \sum_{j=1}^{4} \left(R_i(t_{u,j}) \cdot 1s \right), \tag{3}$$

with $I(u_{end}) = 0$. The total intensity is given by

$$I_{total} = \sum_{u_{start}}^{u_{end}} I_L(u), \tag{4}$$

with the starting position of the collimator jaw u_{start}. Figures 3 to 6 show the normalized beam intensity $I(u)/I_{total}$ versus the collimator jaw position for the different scrapings in B1 and B2. The measurement data (purple) were fitted with the double Gaussian function

$$I_{fit}(u) = I_1 \left(1 - e^{\frac{-(u-\mu)^2}{2\sigma_1^2}} \right) + I_2 \left(1 - e^{\frac{-(u-\mu)^2}{2\sigma_2^2}} \right) \tag{5}$$

with the fit coefficients μ, σ_1, σ_2, I_1 and I_2. The fit is plotted in black and the two terms in green and blue. The fit coefficients for the different scrapings are summarized in table 3. In addition the two last columns of this table show the beam offsets μ as measured in the corresponding primary collimators during the collimation set-up in March 2011 and the differences to the fitted values. In B2 the agreement is better than 210 μm whereas in B1

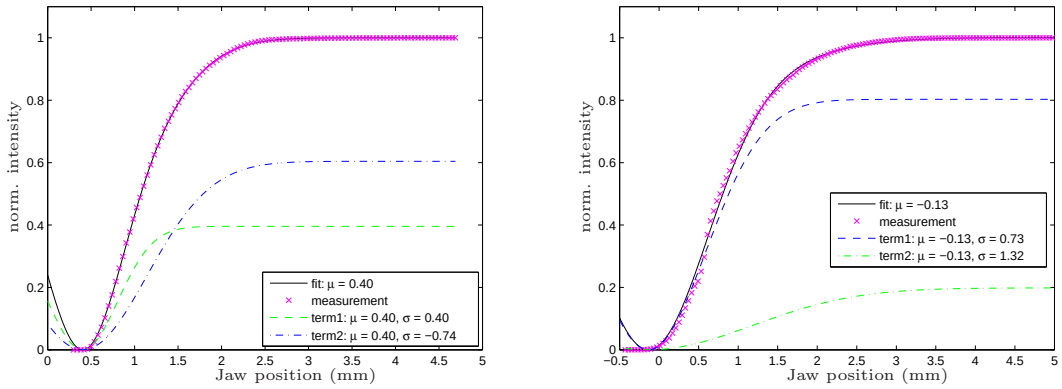

Figure 3: Measured normalized beam intensity $I(u)/I_{total}$ versus collimator jaw position (purple) with a double Gaussian fit (black) and the two terms of the fit function given in equation 5 (green, blue). The fit coefficients are shown in the legend. **Left:** Vertical scraping in B1 with TCP.D6L7.B1. **Right:** Horizontal scraping in B1 with TCP.C6L7.B1.

Table 3: Fit coefficients for the slow scrapings in the different planes and beams. The two last columns show the beam offsets μ as measured in the corresponding primary collimators during the collimation set-up in March 2011 and the differences to the fitted values.

Scraping plane	I_1	I_2	σ_1 [mm]	σ_2 [mm]	μ [mm]	μ [mm] Coll setup	$\Delta\mu$ [mm]
B1 ver	0.396	0.604	0.403	0.74	0.404	0.47	-0.066
B1 hor	0.806	0.195	0.729	1.322	-0.135	-0.31	0.175
B1 skew	0.540	0.460	0.620	1.09	-0.290	-0.64	0.350
B2 ver	0.998	-	0.71	-	0.65	0.65	0.0
B2 hor	0.610	0.390	0.62	1.12	0.050	-0.160	0.210
B2 skew	0.353	0.648	1.29	0.83	-0.619	-0.635	0.016

the agreement is only better then 350 μm. Note that there was no time to confirm the beam centres with a beam based setup of the primary collimators during the MD.

The normalized integrated lost intensity at the collimator jaw position u can be written as

$$I_{tot,lost}(u) = \sum_{u_{start}}^{u} I_L(u)/I_{total}, \tag{6}$$

and is depicted in figure 7. From $I_{tot,lost}(u)$ the population of the beam halo above a certain beam sigma can be derived directly. Tables 4 and 5 summarize the measured fraction of beam intensity in the tails of the beam outside selected multiples of the measured and nominal beam size at 450 GeV.

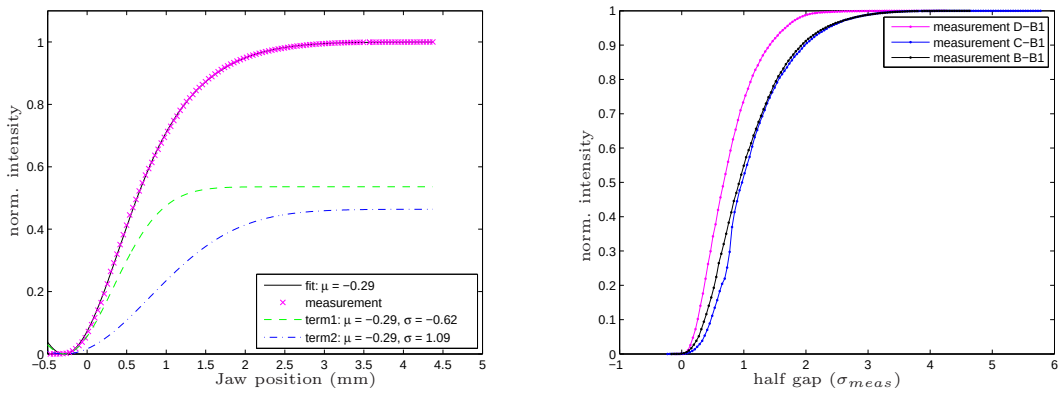

Figure 4: **Left:** Skew scraping in B1 with TCP.B6L7.B1. Measured normalized beam intensity $I(u)/I_{total}$ versus collimator jaw position (purple) with a double Gaussian fit (black) and the two terms of the fit function given in equation 5 (green, blue). The fit coefficients are shown in the legend. **Right:** Comparison of the measured normalized beam intensities $I(u)/I_{total}$ versus the collimator half gap in units of measured beam size, σ_{meas}, for the vertical (purple), horizontal (blue) and skew (black) scrapings in B1. Note: it was assumed $\sigma_{meas} = 0$ for the collimator jaw position $u_i = \mu_{i,0}$, with the fitted beam offset $\mu_{i,0}$ for scraping i.

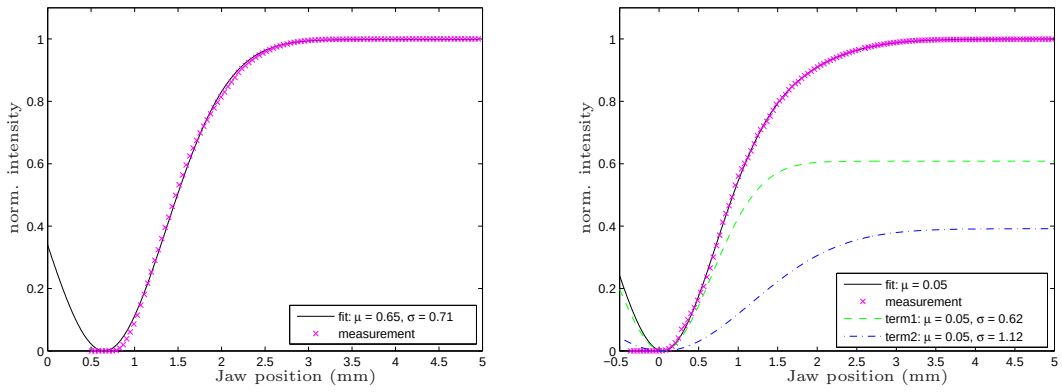

Figure 5: Measured normalized beam intensity $I(u)/I_{total}$ versus collimator jaw position (purple) with a double Gaussian fit (black) and the two terms of the fit function given in equation 5 (green, blue). The fit coefficients are shown in the legend. **Left:** Vertical scraping in B2 with TCP.D6R7.B2. **Right:** Horizontal scraping in B2 with TCP.C6R7.B2.

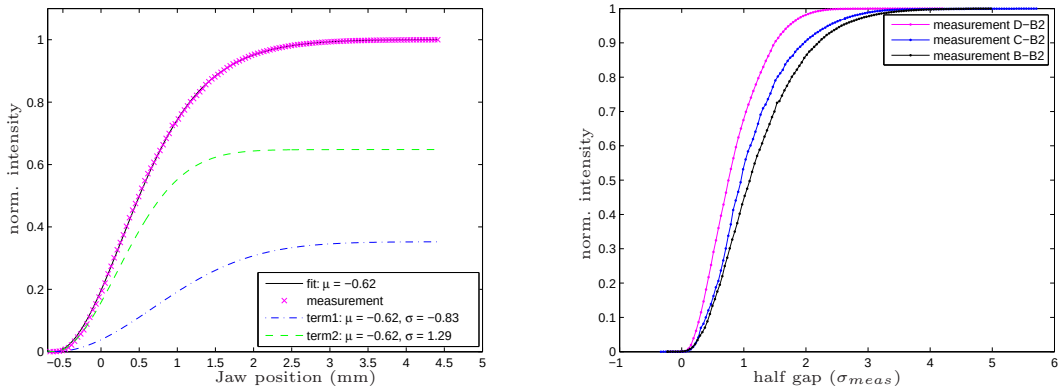

Figure 6: **Left:** Skew scraping in B1 with TCP.B6R7.B2. Measured normalized beam intensity versus collimator jaw position (purple) with a double Gaussian fit (black) and the two terms of the fit function given in equation 5 (green, blue). The fit coefficients are shown in the legend. **Right:** Comparison of the measured normalized beam intensities $I(u)/I_{total}$ versus the collimator half gap in units of measured beam size, σ_{meas}, for the vertical (purple), horizontal (blue) and skew (black) scrapings in B2. Note: It was assumed $\sigma_{meas} = 0$ for the collimator jaw position $u_i = \mu_{i,0}$, with the fitted beam offset $\mu_{i,0}$ for scraping i.

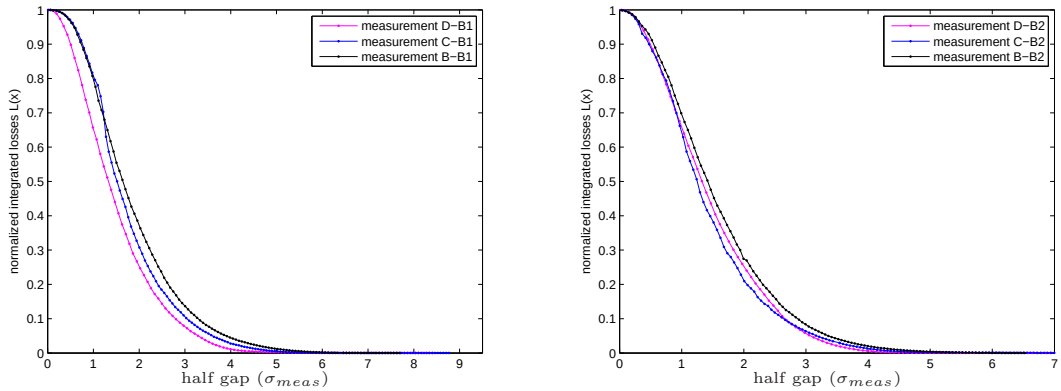

Figure 7: Comparison of normalized integrated lost beam intensity, $I_{tot,lost}(u)/I_{total}$, versus jaw position in units of measured beam sigma, σ_{meas}, during vertical (purple), horizontal (blue) and skew (black) scrapings (left: B1, right: B2). The population of the beam halo above a certain beam sigma can be directly derived from these plots. Note: It was assumed $\sigma_{meas} = 0$ for the collimator jaw position $u_i = \mu_{i,0}$, with the fitted beam offset $\mu_{i,0}$ for scraping i.

Table 4: Measured fraction of beam intensity in the tails of the beam outside selected multiples of the measured beam size, σ_{meas}, at 450 GeV.

u $[\sigma_{meas}]$	$I_{tot,lost}(u)/I_{total}$ vertical	$I_{tot,lost}(u)/I_{total}$ horizontal	$I_{tot,lost}(u)/I_{total}$ skew
	B1	B1	B1
4	9.4e-3	3.8e-2	4.5e-2
5	2.2e-3	7.8e-3	1.3e-2
5.7	8.4e-4	1.6e-3	3.8e-3
6.7	1.8e-4	1.8e-4	4.4e-3
8	2.0e-6	3.3e-5	8.0e-6
8.5	6.2e-8	1.4e-5	9.6e-7
9	-	1.0e-6	-
	B2	B2	B2
4	1.3e-2	1.5e-2	2.77e-2
5	8.9e-4	2.3e-3	5.8e-3
5.7	2.8e-4	1.3e-3	1.65e-3
6.7	3.0e-5	6.6e-4	7.0e-5
8	4.0e-6	1.6e-3	5.0e-6
8.5	5.3e-7	8.0e-6	8.7e-7
9	-	8.5e-7	-

Table 5: Measured fraction of beam intensity in the tails of the beam outside selected multiples of the nominal beam size, σ_{nom}, at 450 GeV.

u $[\sigma_{nom}]$	$I_{tot,lost}(u)/I_{total}$ vertical	$I_{tot,lost}(u)/I_{total}$ horizontal	$I_{tot,lost}(u)/I_{total}$ skew
	B1	B1	B1
3.5	2.74e-3	1.2e-3	1.2e-2
4	8.4e-4	2.3e-4	3.2e-3
4.5	2.4e-4	9.5e-5	1.0e-3
5	5e-5	4.8e-5	2.1e-4
	B2	B2	B2
3.5	3.9e-3	2.7e-3	1.0e-2
4	5.9e-4	1.4e-3	4.7e-3
4.5	1.4e-4	9.2e-4	2.0e-3
5	3.0e-5	4.8e-4	7.0e-4

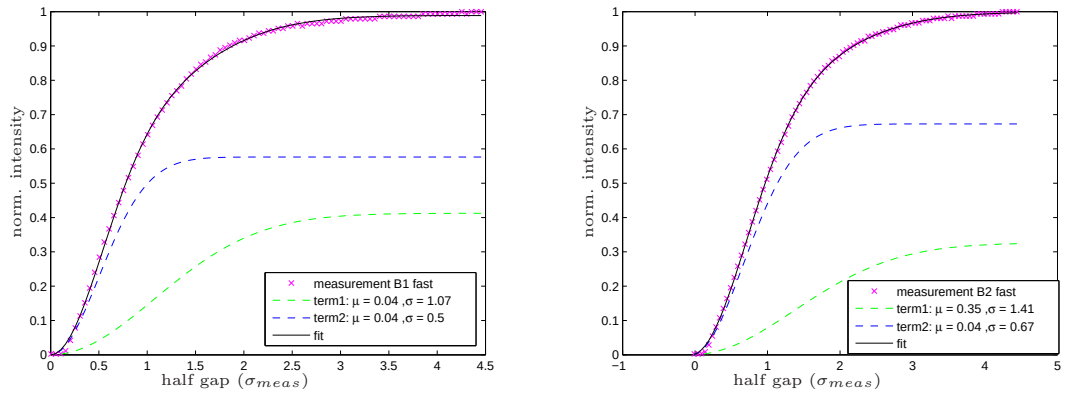

Figure 8: Measured normalized beam intensity $I(u)/I_{total}$ versus collimator jaw position (purple) with a double Gaussian fit (black) and the two terms of the fit function given in equation 5 (green, blue). The fit coefficients are shown in the legend. **Left:** Vertical scraping in B1 with TCP.D6L7.B1. **Right:** Vertical scraping in B2 with TCP.D6R7.B2.

3.2 Fast scraping in the vertical plane

At the end of the MD the beams were scraped away with fast scrapings in the vertical plane. The vertical primary collimators were continuously moved into the beam with a speed of 2 mm/s until the beams were completely scraped away. In parallel the beam intensity was logged with a frequency of 50 Hz. The measured normalized beam intensity versus jaw position in units of measured beam sigma, σ_{meas} is plotted for both beams in figure 8. The measured data were fitted with the function given in equation 5. The fitted function and the two terms are also shown.

The comparison of the measured beam population during the fast and the slow scrapings in the vertical planes of B1 and B2 are depicted in figure 9. It can be clearly seen that the width of the beam distributions measured during the fast scraping is $\sim$ 70 % of the width measured during the slow scrapings. This behaviour can possibly be explained from the previously observed temporal loss tails during beam scrapings with collimators. These temporal tails were also observed during the slow beam scrapings. Figure 10 shows a comparison between the lost particles during each step of the collimator movement, $I_L(u)$ (see equation 2), which are summed over the 4 seconds of the step, and the lost particles per second, $R_i(t) \cdot 1s$, during a slow scraping with the TCP.D6L7.B1. Figure 11 shows the ratio of these two measures. It can be clearly seen that the losses described by $R_i(t) \cdot 1s$ are about $\sim$ 70 % of $I_L(u)$. The physical processes, which cause these temporal tails are currently under investigation. During a fast scraping these temporal tails are not taken into account, which causes a smaller measured width of the measured beam distribution compared to a slow scraping.

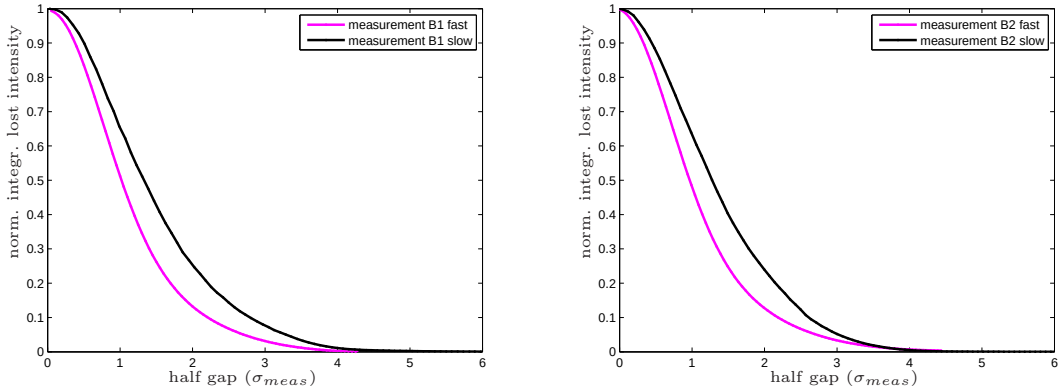

Figure 9: Comparison of the normalized integrated lost beam intensity, $I_{tot,lost}(u)/I_{total}$, versus jaw position in units of measured beam sigma, σ_{meas}, during slow (black) and fast (purple) vertical scrapings (left: B1, right: B2). Note: It was assumed $\sigma_{meas} = 0$ for the collimator jaw position $u_i = \mu_{i,0}$, with the fitted beam offset $\mu_{i,0}$ for scraping i.

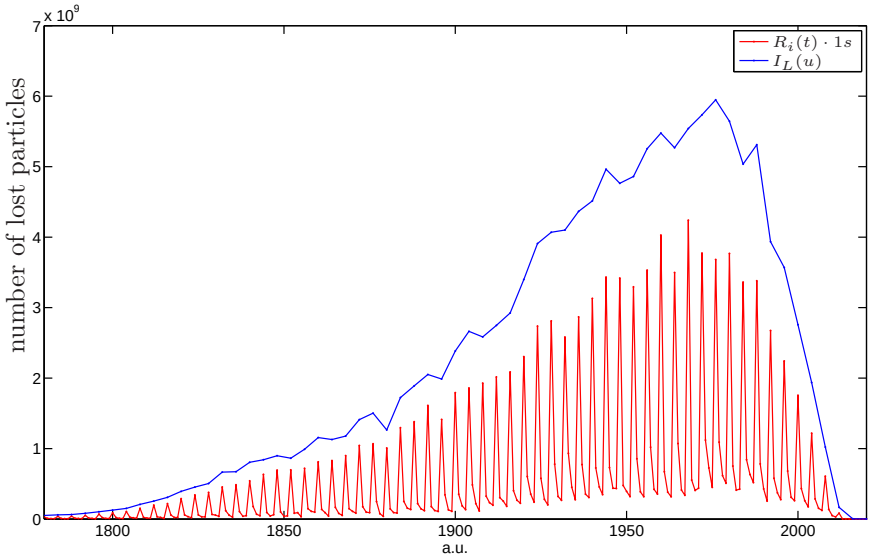

Figure 10: Comparison of the lost intensity at each scraping step, $I_L(u)$, and the intensity lost in a second, $R_i(t) \cdot 1s$, during a slow vertical scraping with the TCP.D6L7.B1.

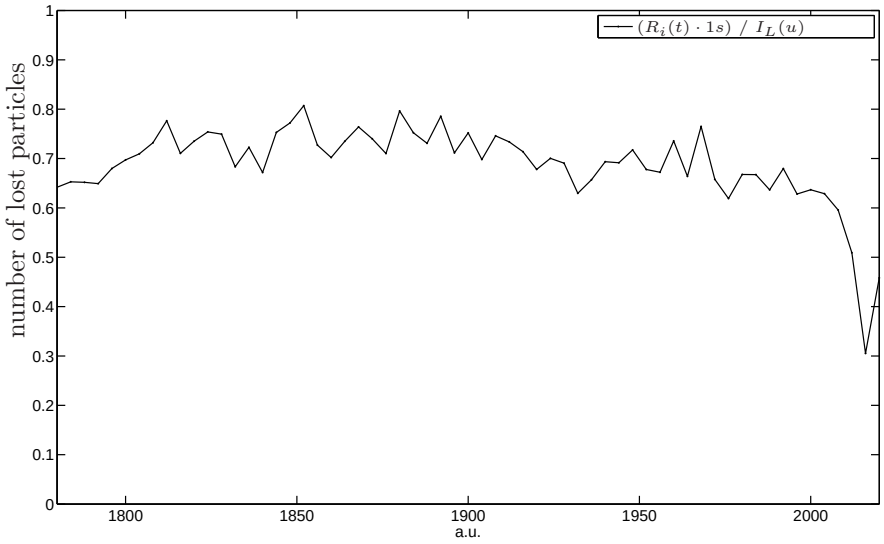

Figure 11: Ratio of the lost intensity at each scraping step, $I_L(u)$, and the intensity lost in a second, $R_i(t) \cdot 1s$, during a slow vertical scraping with the TCP.D6L7.B1.

3.3 Microphone analysis

During the performed scraping tests, two condenser microphones installed close to primary collimators in IR7 for beam 1 have been recorded, c.f. 12. With the microphones being attached to the LHC tunnel walls, they have a distance of approximately 1.5 m to the beam pipes. The acquired data was sampled with 200 ksamples/s and a resolution of 24 bit. The microphones cover a frequency range of 4 Hz to 100 kHz with a dynamic range of 28 – 164 dBSPL. The system is calibrated to factory settings. The purpose of the microphones is to monitor sounds evoked by shockwaves in the collimators. Shockwaves are produced by heavy beam impacts on the collimator jaws. They prolong to the collimator tank through the jaw supports and then propagate to the surrounding air in the LHC tunnel. While it was proven that such sounds evoked during material tests at the SPS in 2004 and 2006 [2], it is subject of current research at which intensity they become detectable with the installed microphones in the LHC, taking into account background noise, distance and radiation impacts. Furthermore, the signals are also observed during normal LHC operation. For LHC operational cycles in early 2011, changes in the spectra of the microphone signals that occurred only during beam losses were seen. In order to qualify these observations, one has to know the location where the loss was created. Therefore, the performed beam scrapings were chosen for a qualitative analysis of the microphone signals.

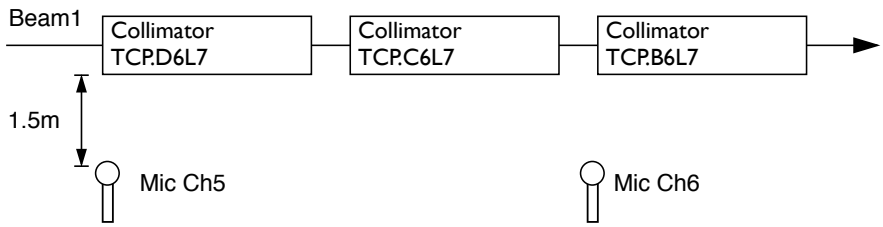

Figure 12: Positions of the microphones installed at the tunnel wall close to primary collimators in IR7 for beam 1.

Stepped scraping at primary collimators in IR7

While moving the collimator jaw towards the beam core with a step of 40 μm every four seconds, spikes in the microphone signals are observed, as can be seen in Fig. 13. The height of the spike's amplitude varies at each scraping step while the shape stays the same. Similar spikes have been observed whenever a sudden rise of the particle loss rate appeared in the BLM signals close to the microphones. It is assumed that such spikes are induced by ionizing radiation in the cables, electronics and the condenser capsule of the microphone itself. However, the low frequency boost created by a spike can easily be filtered with a high pass filter at a cutoff frequency as low as a few Hz.

Another change in the spectra is observed at 11.245 kHz, which corresponds to the beam revolution frequency f_{rev}. Fig. 14 and 15 show the differences of the spectra at the f_{rev} range during normal operation and the scraping. In Fig. 14, only background noise from different parts of the machine in this area and electrically induced noise is seen (not further specified). In Fig. 15, a component in the order of the background noise arises at f_{rev}.

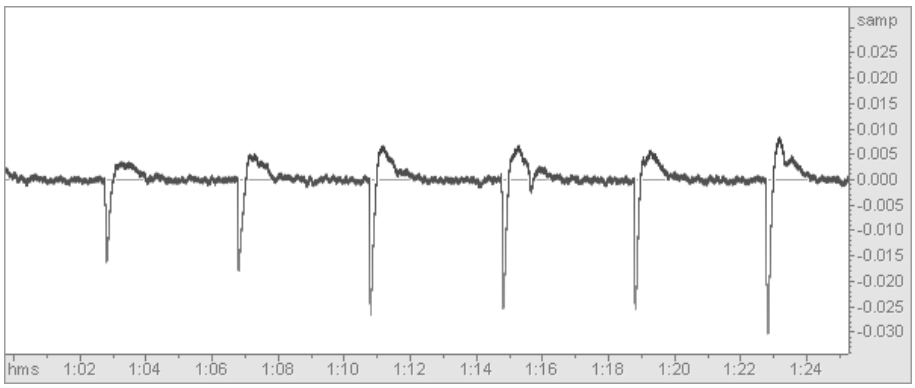

Figure 13: Spikes in microphone signals during stepped scraping, steps every 4s.

Fig. 16 - 18 show a comparison of both microphone channels with the BLM signal at the horizontal collimator as a reference for all three performed scrapings at the vertical (TCP.D6L7), horizontal (TCP.C6L7), and skew (TCP.B6L7) collimator of B1 in IP7. The absolute values of the microphone signals were summed over 1.3s and down-sampled to 1Hz, similar to the BLM data (RS9). The microphone signals are dominated by the low frequency spike at each scraping step. In addition, the sum of three FFT coefficients at f_{rev} and its neighbors are plotted using an FFT length and hop size of 200 kSamples (corresponding to the sampling rate, which results in one value per second and a resolution of one Hz). The microphone signals correspond very well to the BLM data once the shown effects exceed background noise level. The peak of the spikes appear linearly to the BLM signals as well as the component at f_{rev}. Most interestingly, for all scrapings, the seen effects appear by a factor of 5 higher in CH 6, which is installed downstream of collimator TCP.D6L7, c.f. 12.

In Fig. 19 and 20, the FFT coefficients are plotted vs. the BLM signal for the scraping at TCP.D6L7 and TCP.C6L7. Now, the linear dependency of losses and FFT bin height becomes obvious. During the scraping at TCP.D6L7 a higher sensitivity at CH6 downstream of the collimator was observed. For the scraping at TCP.C6L7, only CH 6 has been plotted, since the effect at CH 5 is already covered by background noise.

It is concluded that both effects, the low frequency spike as well as the f_{rev} component, are induced by radiation, since they appear stronger at CH6 for a scraping at TCP.D6L7. CH6 is installed approximately 1.5 m further away and downstream from the impacted collimator, while CH5 is installed at the level of the upstream end of the collimator. Sounds emanating from vibrations of the collimator are assumed to propagate omni-directional from the source, while radiation appears much stronger downstream due to the particles relativistic velocity.

Fast Scraping in the Vertical Plane

The FFT spectrum during the loss spike from a fast scraping at the vertical collimator clearly shows the arising frequency component at f_{rev}, c.f. Fig. 22. For comparison, the FFT spectrum a few seconds later (with no more beam) is shown. Notice, that the difference of the spectra does not cancel out the background noise at high frequencies while it does for frequencies below 3 kHz, this effect was not studied in detail. The collimator is moved

Figure 14: Spectrum during normal operation containing no higher losses. Only background noise from the environment is picked up with the microphone.

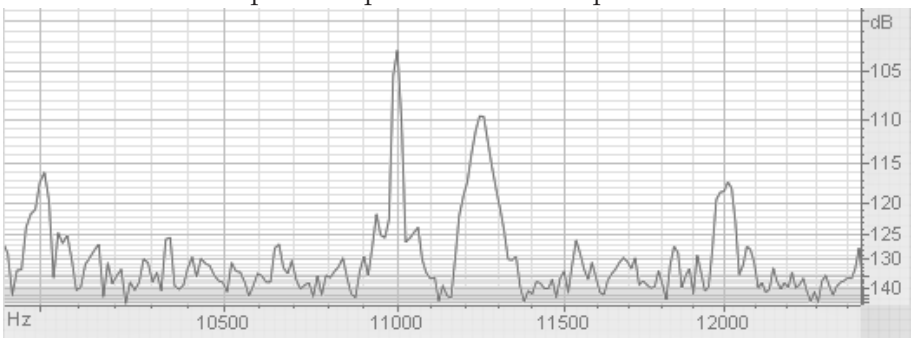

Figure 15: Spectrum during multi-turn loss at primary collimator. A component at the beam revolution frequency $f_{rev} = 11.245\,\text{kHz}$ arrises.

continuously with a speed of 2 mm/s towards the beam core until the beam is fully scraped away. In the low frequency part of the spectra, components at 200 Hz and its harmonics up to 1400 Hz arise, c.f. Fig. 21. These components were recognized as harmonic sounds from the collimator motor movements in an earlier test recording of a collimator on a test bench. While the component at f_{rev} again appears stronger in CH6, the collimator motor movements have similar levels in both Channels. The distance from motor to microphone position is equal for both channels regarding the motor downstream and differs about one meter for the motor upstream. Thus, no big differences in the levels are expected.

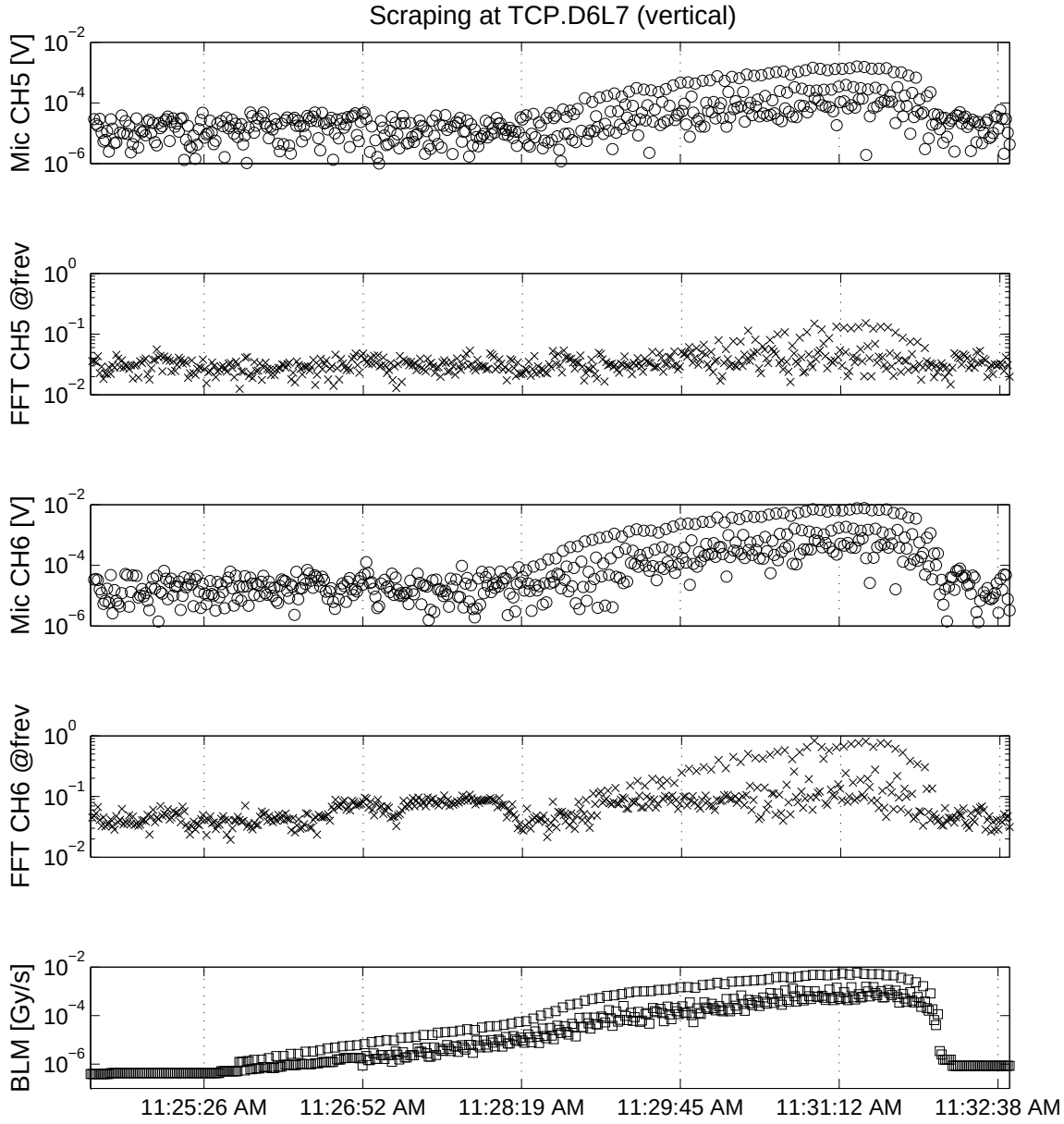

Figure 16: Scraping at TCP.D6L7 vertical collimator. Comparison of the microphone signals CH5 and CH6 (shown are the absolute values summed over 1.3 s and down-sampled to 1 Hz), the corresponding FFT bins at f_{rev}, and the BLM signal at collimator TCP.C6L7 as a reference.

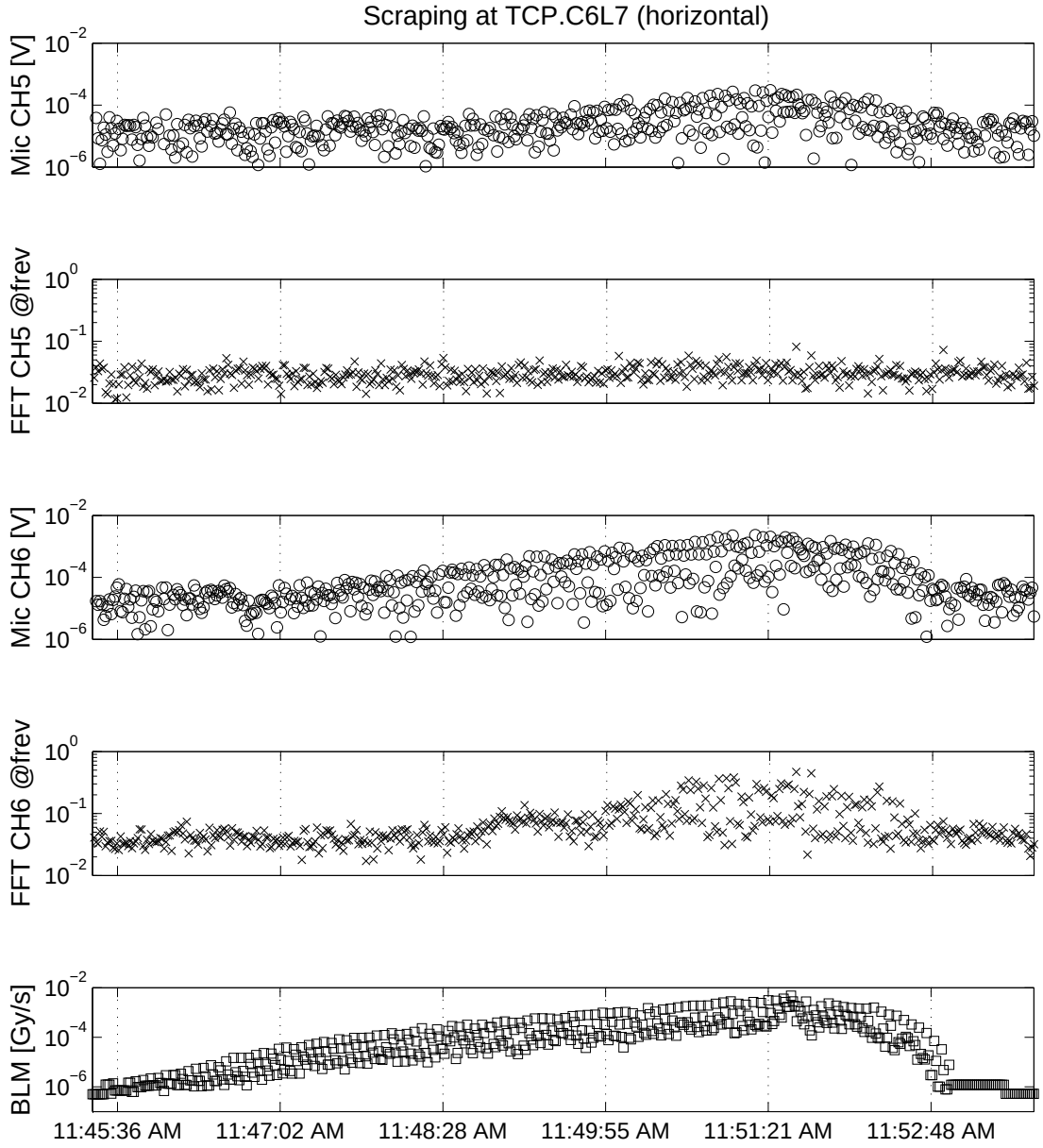

Figure 17: Scraping at TCP.C6L7 horizontal collimator. Comparison of the microphone signals CH5 and CH6 (shown are the absolute values summed over 1.3 s and down-sampled to 1 Hz), the corresponding FFT bins at f_{rev}, and the BLM signal at collimator TCP.C6L7 as a reference.

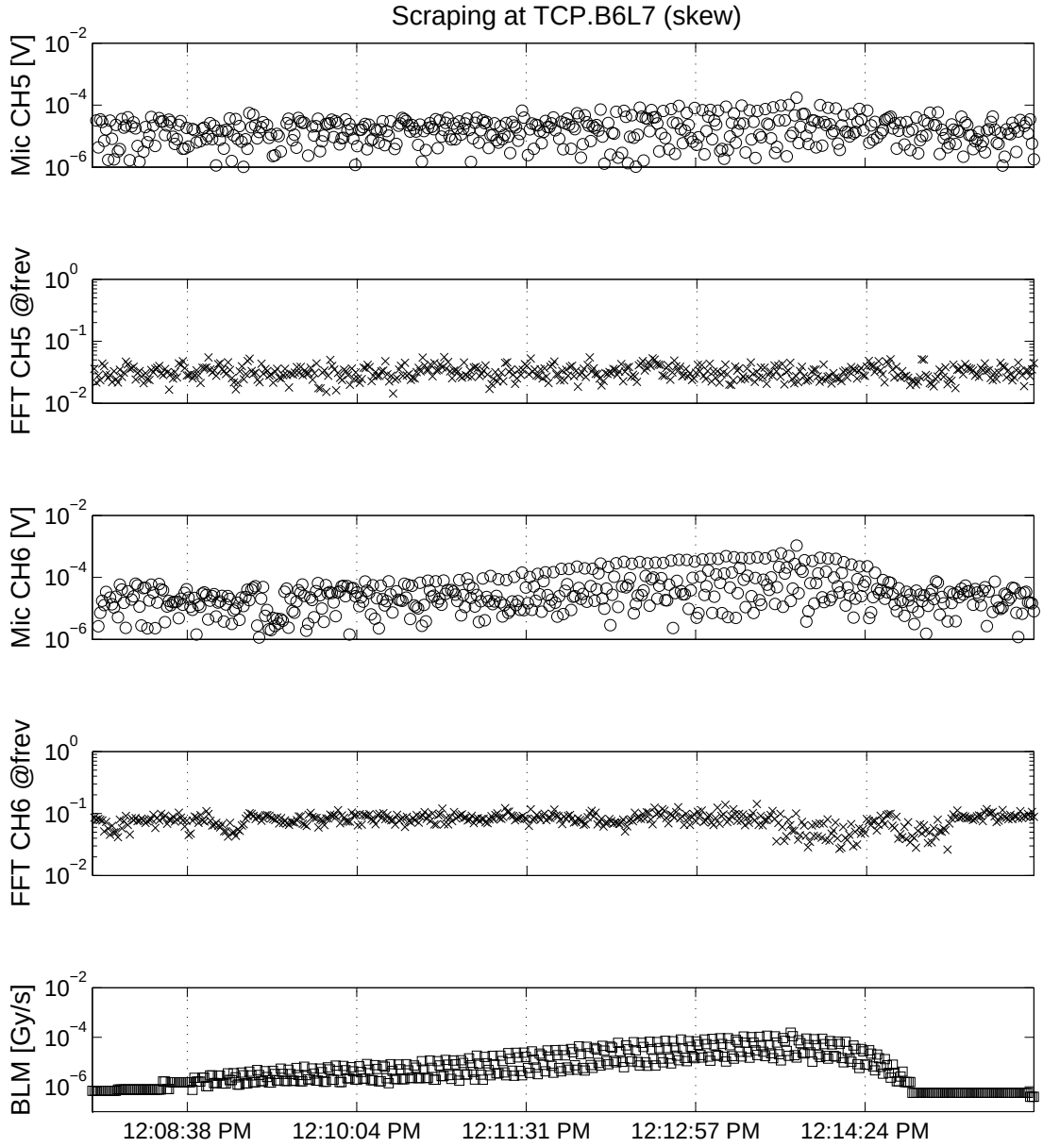

Figure 18: Scraping at TCP.B6L7 skew collimator. Comparison of the microphone signals CH5 and CH6 (shown are the absolute values summed over 1.3 s and down-sampled to 1 Hz), the corresponding FFT bins at f_{rev}, and the BLM signal at collimator TCP.C6L7 as a reference.

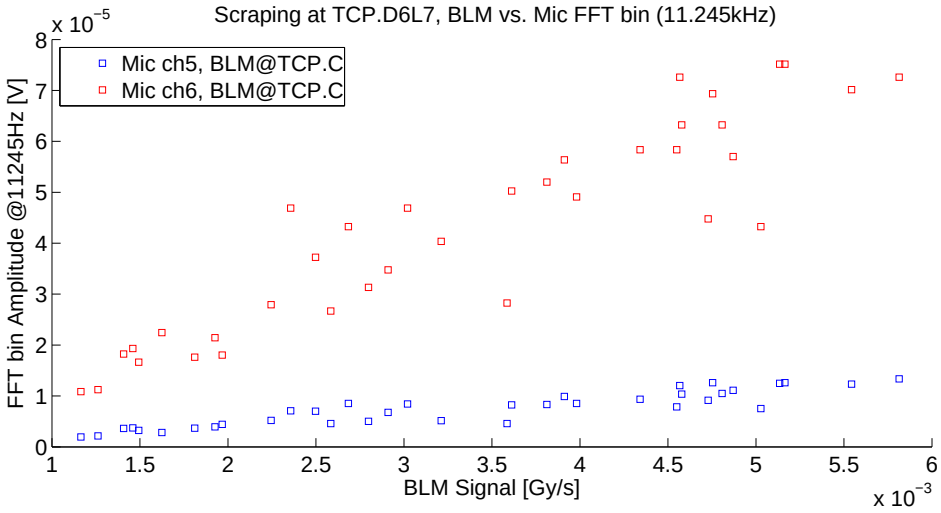

Figure 19: Scraping at TCP.D6L7 vertical collimator,fft size=16384, window=hann. A higher sensitivity to losses can be seen at CH6 downstream of the scraping collimator.

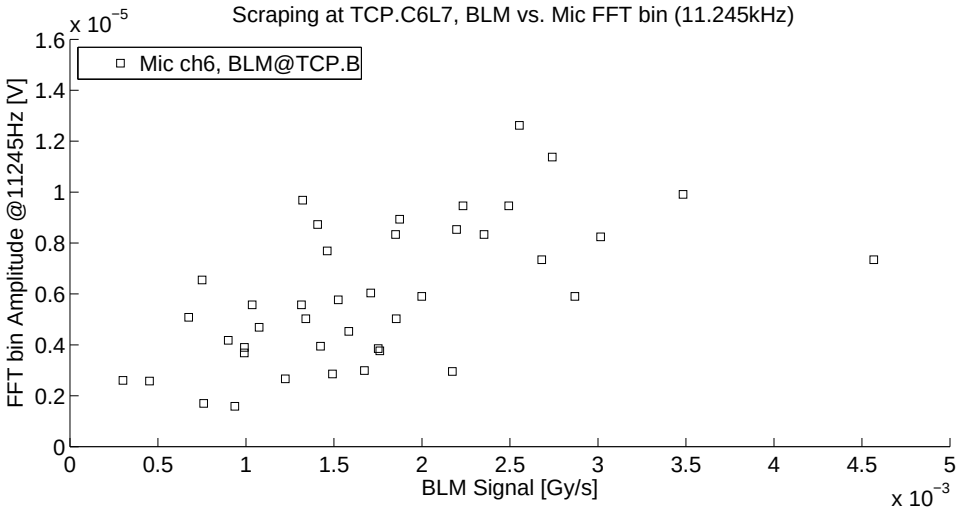

Figure 20: Scraping at TCP.C6L7 horizontal collimator, fft size=16384, window=hann. The signal becomes too noisy for detection in CH5 upstream of the scraping collimator.

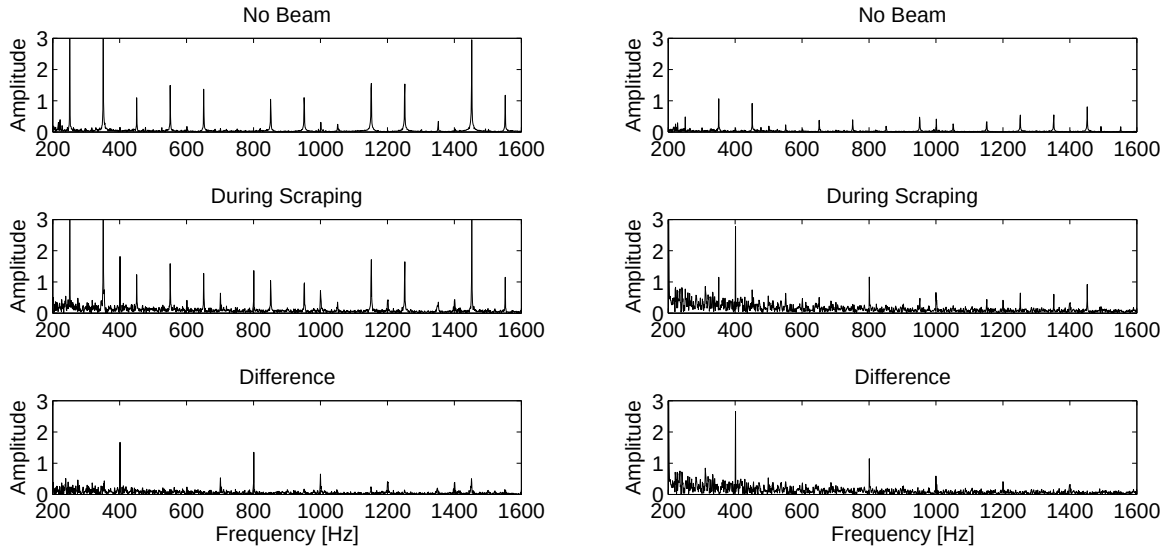

Figure 21: Comparison of spectra at CH5 (left) and CH6 (right), 200-1600Hz frequency range, applied is a 4th order butterworth high pass filter with a cutoff frequency of 200hz. Shown are the spectra after the beam was scraped away (top) and during the fast scraping (middle). The difference of both spectra shows components at $400, 800, 1000, 1200$ and $1400\,\mathrm{Hz}$ coming from the sound of the collimator motor movement (bottom).

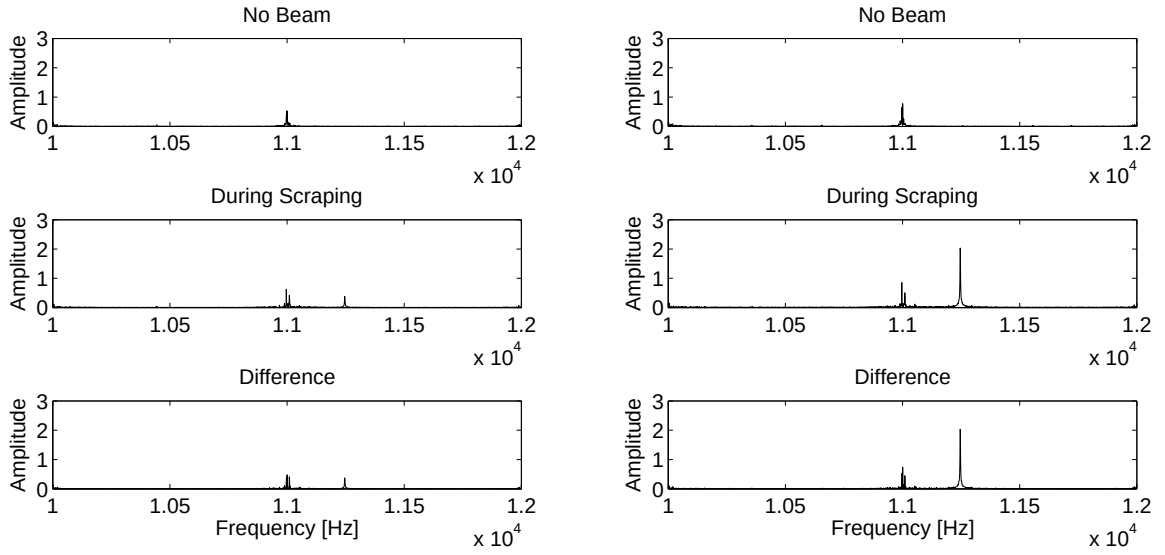

Figure 22: Comparison of spectra at CH5 (left) and CH6 (right), $10 - 12\,\mathrm{kHz}$ frequency range. f_{rev} becomes clearly visible during the fast scraping. Note that the background noise does not cancel out when calculating the difference of both spectra (bottom).

4 Conclusion

For the first time a complete set of slow full beam scrapings was measured in the LHC at 450 GeV. Measurements were performed in the horizontal, vertical and skew planes with the respective primary collimators installed in IR7. The measured intensities were fitted with a double Gaussian function. The measured population of the beam tails are summarized in figure 7 and tables 4 and 5.

A comparison between slow and fast vertical scrapings showed that the width of the measured beam population for the latter is about 70% of the width one measured with the slow scraping. Most probably this is caused by the so-called loss temporal tails, which play a significant role during the slow scraping. The physics processes behind these are currently under investigation.

The scraping losses were also observed with two condenser microphones installed close to the first primary collimators of B1 in IR7. It was shown that the microphone signals are impacted by radiation spikes during losses exceeding approx. 10^{-4} Gy/s. These increase linearly with the loss intensity. The constant ratio between BLM and microphone responses can, thus, be used as scaling coefficient to determine instantaneous loss rates at the collimators directly from the microphone signals. FFT coefficients of the microphone signals at f_{rev} increase linearly with the radiation level. It is concluded that the occurrence of f_{rev} in the microphone spectra is induced by radiation. During this MD no acoustic signals besides the motor sound during the jaw movements were detected with the current microphone installation.

5 Outlook

Due to the limited time of machine availability only a subset of the MD program could be performed. It is therefore proposed to finish the MD program during a future MD. This will be important to confirm the measured beam tail population. In addition this will help to improve the understanding of the differences in the measured width of beam population between slow and fast scrapings.

Further microphone studies will include a comparison of the microphone signal spectra with high sample rate BLM signals. These are for example available for post mortem events. The sampling rate of up to 200kHz of the microphone signals would in principle be sufficient to bunch wise resolve higher particle losses. Assuming that f_{frev} can only occur in the microphone signals for multi-turn losses, one could also distinguish between single-turn losses (only spike) and multi-turn losses (spike + f_{rev}). This will be studied parasitically to normal LHC beam operation and during future (scraping) MDs.

6 Acknowledgments

The authors would like to thank A. Masi, C. Derrez and their team for their help and support in setting up the microphones and in acquiring the microphone data from the tunnel. The authors also would like to thank the colleagues from the CERN OP, BI, BTP and BLM teams for their collaboration, support and helpful discussions.

References

[1] D. Wollmann, R.W. Assmann, G. Bellodi, R. Bruce, M. Cauchi, J.M. Jowett, S. Redaelli, A. Rossi, and G. Valentino. Multi-turn losses and cleaning. In *Proceedings of LHC Beam Operation Workshop, Evian, France*, 2010.

[2] S. Redaelli, O. Aberle, R.W. Assmann, A. Masi, and G. Spiezia. Detecting Impacts of Proton Beams on the LHC Collimators with Vibration and Sound Measurements. In *Proceedings of PAC 2005, Knoxville, Tennessee*, 2005.